

Internal bias effects on pyroelectric measurements near the Curie temperature in triglycine sulphate

A. Shaulov and M. Simhony

Citation: *J. Appl. Phys.* **47**, 1 (1976); doi: 10.1063/1.322344

View online: <http://dx.doi.org/10.1063/1.322344>

View Table of Contents: <http://jap.aip.org/resource/1/JAPIAU/v47/i1>

Published by the [American Institute of Physics](#).

Related Articles

Electro-caloric effect in $0.45\text{BaZr}_{0.2}\text{Ti}_{0.8}\text{O}_3\text{-}0.55\text{Ba}_{0.7}\text{Ca}_{0.3}\text{TiO}_3$ single crystal
Appl. Phys. Lett. **102**, 082902 (2013)

Interferometric measurement of the pyroelectric coefficient in lithium niobate
J. Appl. Phys. **113**, 043101 (2013)

Dielectric and enhanced pyroelectric properties of $(\text{Pb}_{0.325}\text{Sr}_{0.675})\text{TiO}_3$ ceramics under direct current bias field
Appl. Phys. Lett. **101**, 262901 (2012)

The study of dielectric, pyroelectric and piezoelectric properties on hot pressed PZT-PMN systems
AIP Advances **2**, 042170 (2012)

Contribution of an extrinsic mechanism for the electrical polarization in BiMn_2O_5 ceramics
AIP Advances **2**, 042165 (2012)

Additional information on J. Appl. Phys.

Journal Homepage: <http://jap.aip.org/>

Journal Information: http://jap.aip.org/about/about_the_journal

Top downloads: http://jap.aip.org/features/most_downloaded

Information for Authors: <http://jap.aip.org/authors>

ADVERTISEMENT



AIP Advances

Now Indexed in Thomson Reuters Databases

Explore AIP's open access journal:

- Rapid publication
- Article-level metrics
- Post-publication rating and commenting

Internal bias effects on pyroelectric measurements near the Curie temperature in triglycine sulphate

A. Shaulov

Physics Department, Ben-Gurion University, Beer-Sheva, Israel

M. Simhony

The Racah Institute of Physics, Hebrew University, Jerusalem, Israel

(Received 9 April 1975; in final form 2 June 1975)

Simultaneous measurements of the pyroelectric (PE) coefficient λ and permittivity ϵ from the PE voltage responses to step infrared radiation signals in triglycine sulphate (TGS) are reported as functions of temperature in both the ferroelectric and paraelectric phases. It is shown that the observed lowering and widening of the peaks of λ and ϵ , the appearance of a PE effect in the paraelectric phase, and the shift of the ϵ peak to temperatures above T_c can be explained by the existence of an internal bias field E_b . The values of E_b calculated to fit the experimental results vary in different TGS samples from 30 to 150 V/cm.

PACS numbers: 77.70., 77.20.

I. INTRODUCTION

The appearance of the pyroelectric (PE) effect above the Curie temperature T_c in triglycine sulphate (TGS) was first reported by Chynoweth¹ and ascribed to space-charge polarization in the crystals. It was also observed in TGS^{2,3} that the permittivity ϵ reaches maximum at a temperature $T_{\epsilon m}$ which is 0.2–0.5 °C higher than the temperature $T_{\lambda m}$, at which the PE coefficient λ has a maximum. Here we report simultaneous measurements of λ and ϵ from PE voltage responses to step infrared radiation signals³ in TGS around T_c . The irregularities in the behavior of λ and ϵ are explained by the influence of an internal bias,^{4–6} based on the thermodynamic theory of a second-order ferroelectric phase transition.^{9,10}

II. CALCULATION OF λ AND ϵ

Consider a ferroelectric crystal with a second-order phase transition to which an electric bias field E_b is applied parallel to the polarization vector \mathbf{P} . For temperatures T close to T_c and in the absence of external pressure, the thermodynamic theory^{9,10} yields

$$[(T - T_c)/\epsilon_0\gamma]P + \eta P^3 - E_b = 0, \quad (1)$$

where $\epsilon_0 = 8.85 \times 10^{-12}$ F/m, γ is the Curie-Weiss coefficient, and η is a positive constant. The PE coefficient $\lambda = |dP/dT|$ is, therefore,⁴

$$\lambda = P/(T - T_c + 3\epsilon_0\gamma\eta P^2) \quad (2)$$

and for the relative dielectric constant ϵ , $\epsilon = \epsilon_0^{-1}(dP/dE)$, one obtains⁵

$$\epsilon = \gamma/(T - T_c + 3\epsilon_0\gamma\eta P^2). \quad (3)$$

Taking $d\lambda/dT$ it was shown⁴ that λ has a maximum value λ_m ,

$$\lambda_m = (3\epsilon_0\gamma\eta^{2/3} E_b^{1/3})^{-1} \quad (4)$$

at $T = T_c$, i. e., $T_{\lambda m} = T_c$, independent of bias.⁴ Unlike this, ϵ has a maximum value⁵ (assuming $3/2^{1/3} \approx 2.4$)

$$\epsilon_m = (2\epsilon_0\eta^{1/3} E_b^{2/3})^{-1} \quad (5)$$

at a temperature $T_{\epsilon m}$ higher than T_c ,

$$T_{\epsilon m} - T_c = 1.2\epsilon_0\gamma\eta^{1/3} E_b^{2/3}. \quad (6)$$

Thus, the bias field shifts $T_{\epsilon m}$ away from $T_{\lambda m} = T_c$ by an amount proportional to $E_b^{2/3}$.

Under the condition

$$E_b \ll (|T - T_c|/\epsilon_0\gamma\eta^{1/3})^{3/2}, \quad (7)$$

Eq. (1) has the linear solutions

$$P = P_s(T) + \epsilon_0\gamma E_b/2(T_c - T), \quad T < T_c \quad (8)$$

$$P = \epsilon_0\gamma E_b/(T - T_c), \quad T > T_c,$$

while always $P(T = T_c) = (E_b/\eta)^{1/3}$ [Eq. (1)]. Here $P_s = P(E_b = 0)$ is the spontaneous polarization,

$$|P_s| = [(T_c - T)/\epsilon_0\gamma\eta]^{1/2}, \quad T < T_c \quad (9)$$

$$|P_s| = 0, \quad T \geq T_c.$$

With Eqs. (7) and (8) one has

$$\lambda = \lambda_0 - \epsilon_0\gamma E_b/2(T_c - T)^2, \quad T < T_c \quad (10)$$

$$\lambda = \epsilon_0\gamma E_b/(T - T_c)^2, \quad T > T_c,$$

where

$$\lambda_0 \equiv \left| \frac{dP_s}{dT} \right| = \frac{1}{2} \left(\frac{\epsilon_0\gamma\eta}{T_c - T} \right)^{1/2}. \quad (11)$$

Thus, below T_c , far enough to satisfy Eq. (7), λ rises with T almost as λ_0 , i. e., proportional to $(T_c - T)^{-1/2}$. Above T_c , far enough again to fulfill Eq. (7), λ decreases as $(T - T_c)^{-2}$. At $T = T_c$, the rising and falling branches of λ meet having the value λ_m . With Eqs. (7) and (8) one also has

$$\epsilon = \gamma/2(T_c - T), \quad T < T_c \quad (12)$$

$$\epsilon = \gamma/(T - T_c), \quad T > T_c,$$

i. e., ϵ is independent of E_b and obeys the Curie-Weiss law. Reversing Eq. (7) one finds that the linear approximation applies for temperatures

$$|T - T_c| \gg \epsilon_0\gamma\eta^{1/3} E_b^{2/3}. \quad (13)$$

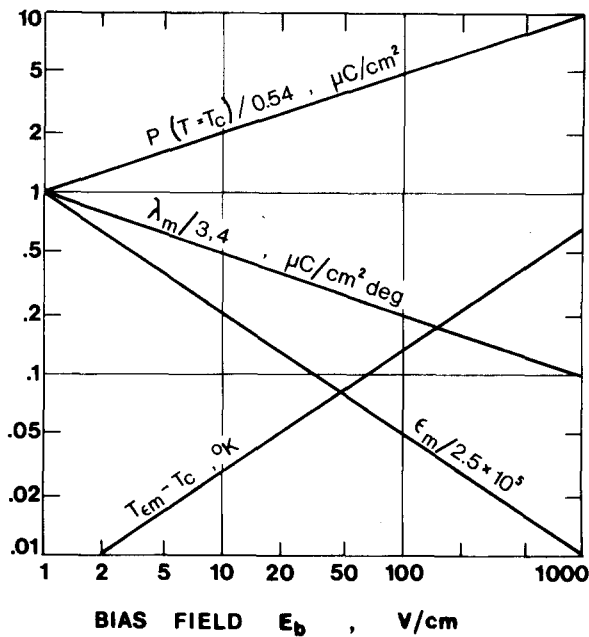


FIG. 1. Bias dependence of $P(T = T_c)$, λ_m , ϵ_m , and T_{em} calculated for TGS.

Comparison with Eq. (6) shows that in the paraelectric phase the linear approximation [Eqs. (8), (10), (12)] applies for temperatures above T_{em} .

In TGS one has $\gamma = 3200^\circ\text{K}$, $\eta = 6.5 \times 10^{11} \text{ J m}^5/\text{C}^4$, and $T_c = 49.5^\circ\text{C}$,³ so that, with E_b in V/cm,

$$P(T = T_c) = 0.54 E_b^{1/3}, \quad \mu\text{C}/\text{cm}^2$$

$$\lambda_m = 3.4 E_b^{-1/3}, \quad \mu\text{C}/\text{cm}^2 \text{ deg}$$

$$\epsilon_m = 2.5 \times 10^5 E_b^{-2/3},$$

$$T_{em} - T_{\lambda m} = 6.3 \times 10^{-3} E_b^{2/3}, \quad ^\circ\text{K}.$$

These parameters are plotted in Fig. 1 against E_b . The linear approximation applies for $E_b \ll 2600 |T_c - T|^{3/2}$ V/cm or, in the paraelectric phase, for temperatures $T - T_c$ lying above the $T_{em} - T_c$ line [Eq. (13)]. The derived equations and parameter values were used to compute P , λ , and ϵ in TGS under bias fields of 0, 50, 250, and 1000 V/cm. Results are presented graphically as functions of $T - T_c$ in Fig. 2.

III. EXPERIMENTAL TECHNIQUE

Measurements were carried out on six samples of single-crystalline TGS with major faces oriented perpendicular to the PE axis and provided with ir transparent electrodes (evaporated InSb). The thickness L of the samples was 15–70 μm , and their electroded radiation-receiving area A was 0.5–4 mm^2 . Attached to the electrodes were 8- μm thin leads of stainless steel which also served as suspenders. The samples were placed in a small oven with a CdS window. The oven was thermistor controlled with temperature stability better than 0.05 $^\circ\text{C}$. The temperature of the sample was measured to $\sim 0.1^\circ\text{C}$ with a calibrated thermocouple attached very close to the rear electrode. The whole mount was held

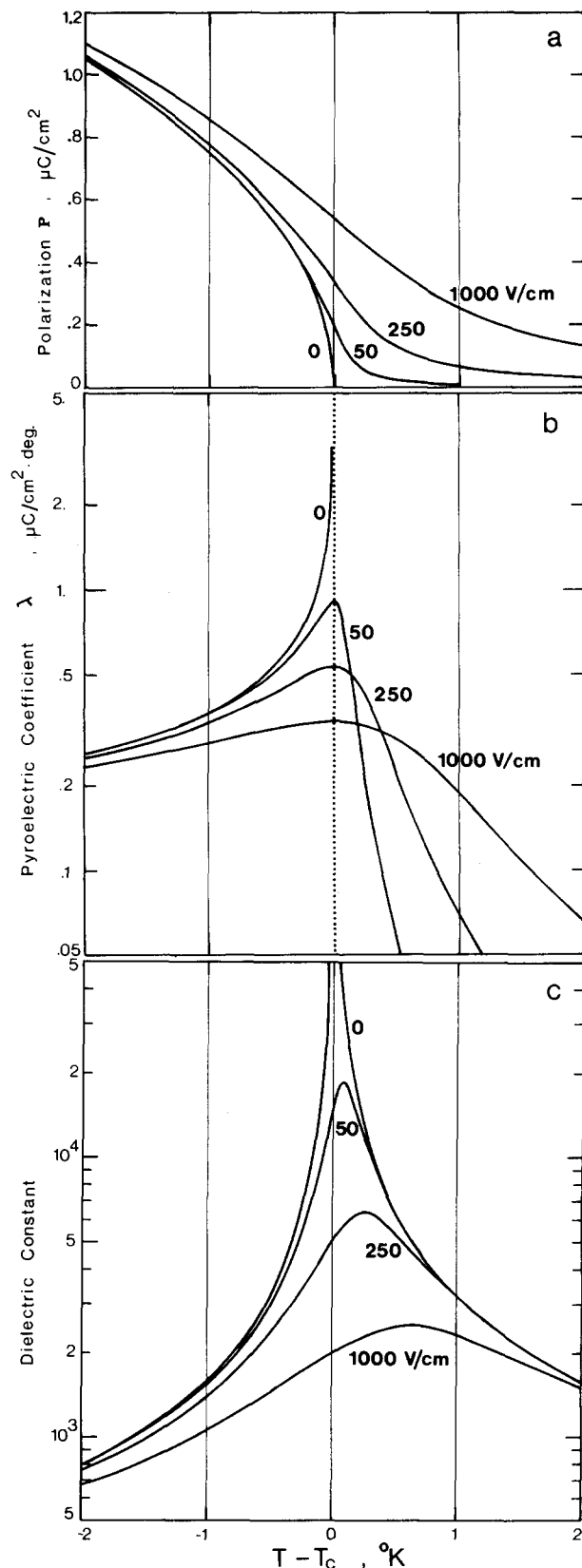


FIG. 2. Computed temperature dependence of P , λ , and ϵ in TGS under bias of 0, 50, 250, and 1000 V/cm.

in a vacuum-tight (up to 10^{-6} Torr) cryostat with a KBr window, in which the sample could be poled in a field up to 10^4 V/cm.

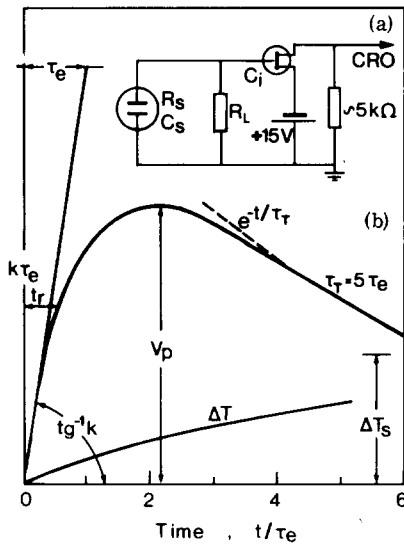


FIG. 3. (a) Measuring circuit. (b) Schematic PE voltage response to a step ir signal for $\theta = 0.2$; ΔT is the exponential temperature rise of the sample during the signal to the saturation value ΔT_s , with time constant τ_T .

The radiation source was a 500 °K blackbody with a shutter fast enough to provide step signals. The measuring circuit consisted of interchangeable load resistors R_L (10^5 – $10^7 \Omega$) connected parallel to the sample and to a FET source-follower circuit, as shown in Fig. 3(a). R_L was small to keep the measured electronic time constant $\tau_e \approx R_L C$ much smaller than the thermal time constant τ_T of the sample, which was 0.5–3 sec. A larger value of R_L may also introduce an additional bias due to the backward current through the FET. For example, a 10^{-11} -A flow on $R_L = 10^{10} \Omega$ would yield ~ 50 V/cm on our samples. The PE response transients were displayed on a Tektronix RM 564 storage CRO with a 3A9 amplifier of usable sensitivity 50 μ V/cm.

A schematic PE voltage response³ is shown in Fig. 3(b). The measured ratio $\theta \approx \tau_e/\tau_T$ is 0.2. The measured parameters of the response are the initial slope k , the peak value V_p , the rise time $t_r \approx \tau_e$, and the fall time $t_f \approx \tau_T$.¹¹ From these parameters λ and ϵ are calculated with the use of relations³

$$\epsilon = \left(\frac{L}{\epsilon_0 A R_L} \right) \tau_e, \quad \lambda = \left(\frac{cL}{F A R_L} \right) V_p, \quad \text{and} \quad \frac{\lambda}{c \epsilon_0 \epsilon} = \frac{k}{F}, \quad (14)$$

where F is the radiation flux absorbed in the sample and c is the volume specific heat. The measurement is valid under the small-signal condition³

TABLE I. Data for Fig. 5.

Line	I	II	III
Internal bias (V/cm)	30	40	150
Sample	T-18	T-20	Z-3
Thickness (μ m)	60	20	40
Area (mm^2)	4	3.3	2
τ_T (sec)	2.4	1.5	2.2
ΔT_s (°K)	0.07	0.12	0.1

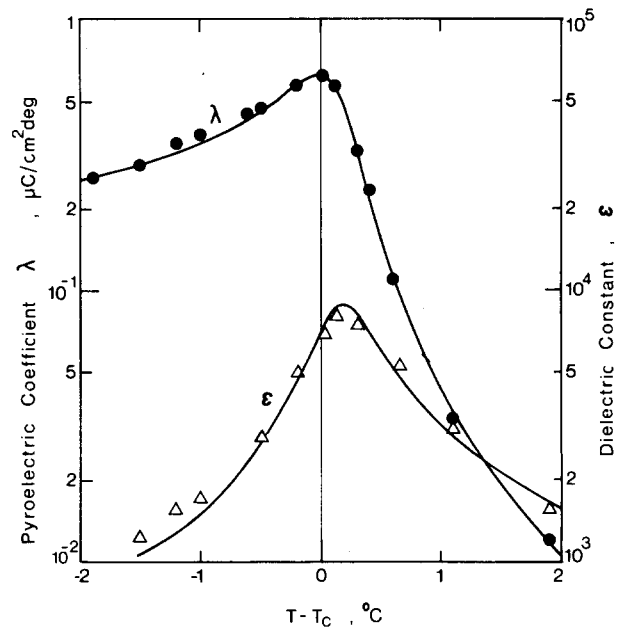


FIG. 4. Experimental values of λ (circles) and ϵ (triangles) as function of temperature. The theoretical λ and ϵ curves are computed for $E_b = 150$ V/cm.

$$\theta \Delta T_s \ll |T_c - T|, \quad (15)$$

where ΔT_s is the saturation value of the exponential temperature rise of the sample during the radiation signal, as shown by the lower curve of Fig. 3. The values of c in TGS are taken from the literature¹² (in the interval under consideration c varies between 2.2

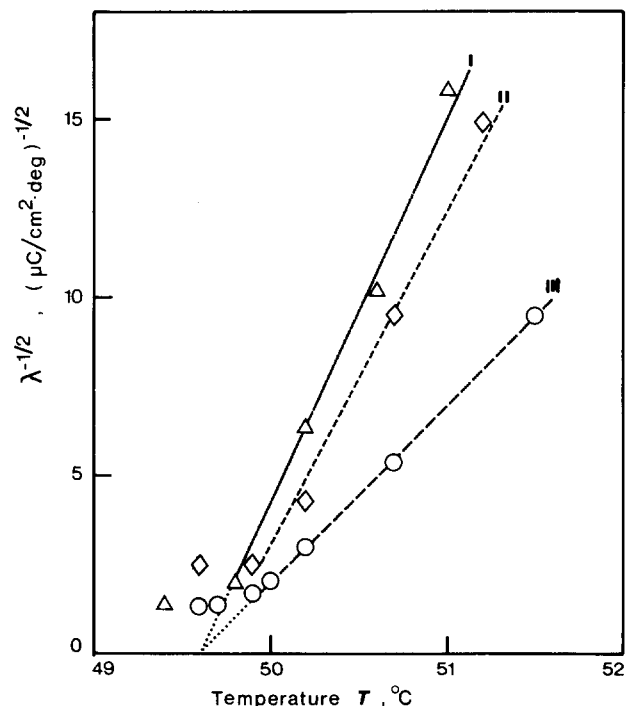


FIG. 5. Experimental $\lambda^{-1/2}$ values in three TGS samples as functions of temperature in the paraelectric phase. The straight $\lambda^{-1/2}$ lines are calculated with $E_b = 30, 40,$ and 150 V/cm. Other details are shown in Table I.

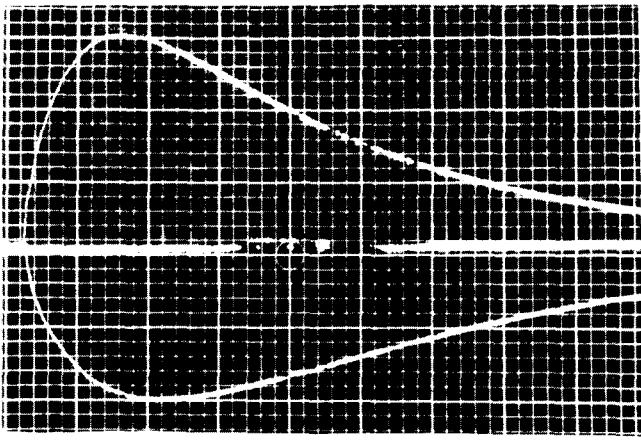


FIG. 6. Oscillogram of the PE voltage response to a step ir signal (upper trace) and of the response to a following step *dark* signal (lower trace) in a TGS sample in the paraelectric phase. $T = 49.7^\circ\text{C}$, $R_L = 10^7 \Omega$; vertically 5 mV/div, horizontally 0.5 sec/div.

and $2.6 \text{ J/cm}^3 \text{ deg}$). However, c can also be calculated using³ $c = (F/L)(\tau_T/\Delta T_s)$, which also yields $\lambda = \tau_T V_p / \Delta T_s A R_L$.

IV. EXPERIMENTAL RESULTS

Values of λ and ϵ obtained from PE voltage responses to step ir signals in a TGS sample without external bias are plotted in Fig. 4 against $T - T_c$ in an interval $\pm 2^\circ\text{C}$ from T_c . The solid lines are λ and ϵ curves computed similarly to the curves of Fig. 1, but with $E_b = 150 \text{ V/cm}$. It is seen that the experimental values of λ (circles) and ϵ (triangles) fit well the corresponding theoretical curves, suggesting that there exists in the sample an internal bias field of $\sim 150 \text{ V/cm}$. The experimentally observed shift $T_{\epsilon_m} - T_{\lambda_m}$ is $\sim 0.2^\circ\text{C}$, which also corresponds to a similar bias.

Experimental values of $\lambda^{-1/2}$ in the *paraelectric* phase in the sample of Fig. 4 and two other TGS samples are plotted against temperature in Fig. 5. It is seen that, except for the closest vicinity of T_c , the experimental points for each sample lie on the theoretical $\lambda^{-1/2}$ straight lines calculated from Eq. (10) with $E_b = 150, 40,$ and 30 V/cm , respectively, suggesting the existence of such internal bias fields in these samples.

An interesting result of the shift between T_{ϵ_m} and T_{λ_m} is seen in Fig. 6. The upper oscillogram here is the PE response to a step ir signal in a TGS sample in the paraelectric phase, 0.2°K above T_c . The signal was followed by a step *dark* signal, the response to which is shown by the lower trace. The two traces are not symmetrical because during the radiation-on signal the sample is heated so that at the beginning of the dark signal λ should be smaller. This results in the observed smaller value of V_p , in accordance with Eq. (14). The longer rise time of the dark response means that ϵ is larger than at the beginning of the radiation signal. But this is possible only if the initial temperatures for both signals are still below T_{ϵ_m} , i.e., that both responses occur in the temperature interval between T_{λ_m} and T_{ϵ_m} .

The response to the light signal is seen to decay faster. Obviously, due to the temperature rise during the signal λ decreases helping to reduce the height of the response. During the dark signal, due to the cooling of the sample, λ increases delaying the fall of the response.

V. DISCUSSION AND CONCLUSIONS

Based on the thermodynamic theory of a second-order ferroelectric phase transition^{9,10} and on the works in Colemanite crystals,⁴⁻⁷ we have calculated the effects of an electric bias field on the polarization, pyroelectric coefficient, and permittivity in TGS around the Curie temperature in the ferroelectric and paraelectric phases. Because of the bias, the polarization does not vanish at the Curie point, but continues to higher temperatures. The pyroelectric coefficient reaches a lower maximum at $T = T_c$, but does not vanish thereafter and is a continuous function of T in the paraelectric phase. The dielectric constant, too, has a lower maximum, occurring above T_c , the further the stronger the field. Because under bias the peaks of λ and ϵ become lower and wider, the transition between the paraelectric and ferroelectric phases is obscured. All these effects were observed in our measurement of λ and ϵ from PE voltage responses to step ir radiation signals in TGS crystals *without* external bias, and we have shown that they can be adequately explained by the action of internal bias fields. The values of the internal bias calculated to fit the experimental results vary in different samples from 30 to 150 V/cm , and could change after heating the samples above T_c and recooling. Other measurements of E_b out of hysteresis loops⁸ in TGS have yielded similar values of $\sim 40 \text{ V/cm}$, while alanine-doped samples had internal bias fields of $\sim 10^5 \text{ V/cm}$.

The continuation of P and λ above T_c was previously observed⁴ in Colemanite and GASH crystals and explained by an internal bias causing a shift of the hysteresis loop.^{4,7} Similarly, the appearance of ϵ_m above T_c and the deviation of ϵ from the Curie-Weiss law in Colemanite were explained, too, by an internal bias.^{5,6} Our measurements from PE responses yield simultaneously the bias effects on both λ and ϵ , thus also the shift between their maxima. The PE measurements do not require the application of external fields and so affect the internal bias much less than hysteresis loop measurements, especially around T_c . It has been suggested⁸ that the internal bias depends on the purity of the samples and that it should not exist in perfect TGS crystals. Such an assumption is reasonable in view of our experience; however, a definite answer cannot be given on the basis of this work, requiring samples of sufficiently more grades of perfection and a deep insight into the history of their growth, thermal and electrical treatment, and an account of possible diffusion of electrode material.

¹A.G. Chynoweth, Phys. Rev. **117**, 1235 (1960).

²L.S. Kremenchugskii and V.B. Samoilov, Sov. Phys.-Solid State **12**, 940 (1968); M.D. Kladkevich, L.S. Kremenchugskii, and A.F. Mal'nev, Ukr. Phys. J. **13**, 442 (1968).

- ³M. Simhony and A. Shaulov, *Appl. Phys. Lett.* **21**, 375 (1972).
- ⁴E. Fatuzzo, *J. Appl. Phys.* **31**, 1029 (1960).
- ⁵H.H. Wieder, *J. Appl. Phys.* **30**, 1010 (1959).
- ⁶H.H. Wieder, A.R. Clawson, and C.R. Parkerson, *J. Appl. Phys.* **33**, 1720 (1962).
- ⁷W.J. Merz, in *Progress in Dielectrics* (Heywood & Co., London, 1962), Vol. 4, pp. 133.
- ⁸E.T. Keve, K.L. Bye, P.W. Whipps, and A.D. Annis, *Ferroelectrics* **3**, 39 (1971).
- ⁹A.F. Devonshire, *Adv. Phys.* **3**, 85 (1954).
- ¹⁰F. Jona and G. Shirane, *Ferroelectric Crystals* (Pergamon, London, 1962), pp. 30–35; E. Fatuzzo and W.J. Merz, *Ferroelectricity* (North-Holland, Amsterdam, 1967).
- ¹¹M. Simhony, A. Shaulov, and A. Maman, *J. Appl. Phys.* **44**, 2464 (1973).
- ¹²J.A. Gonzalo, *Phys. Rev. Lett.* **21**, 749 (1968); M.J. Tello and J.A. Gonzalo, *J. Phys. Soc. Jpn. Suppl.* **28**, 199 (1970); S.A. Taraskin, B.A. Strukov, and V.A. Meleshina, *Sov. Phys.-Solid State* **12**, 1089 (1970).